

## The positive temperature anomaly as detected by Landsat TM data in the eastern Marmara Sea (Turkey): possible link with the 1999 İzmit earthquake

M. T. YÜRÜR

Hacettepe University, Department of Geological Engineering, 06532, Beytepe Campus, Ankara, Turkey; e-mail: tyurur@hacettepe.edu.tr

(Received 2 March 2005; in final form 18 May 2005)

A long (~15 km) and narrow (~4 km) offshore positive temperature anomaly (~1.7° C) is observed in the Landsat Thematic Mapper (TM) thermal infrared (TIR) image acquired the day following the large İzmit earthquake (Mw 7.4) of 17 August 1999, in eastern Marmara Sea, Turkey. The earthquake was generated along the North Anatolian Fault, which ruptured for about 150 km, and the anomaly formed at the western termination of this rupture. Discussions of this anomaly may develop by processes different than the seismic activity and considerations on fault geometry and sea bathymetry characteristics suggest that the anomaly may result from aftershock activity near the western end of the earthquake fault. The formation of the anomaly requires the addition of a large quantity of hot waters to the sea. The ascent to the sea bottom of fault-driven hot fluids (seismic pumping) and formation of thermal plumes may be the processes by which the sea surface temperature increased. Recent works and the present study suggest that TIR data analysis may be used as a tool in seismological studies.

### 1. Introduction

A strong earthquake (Mw 7.4) struck the Gulf of İzmit at the eastern part of the Marmara Sea on 17 August 1999, at about 03 a.m. local time (figure 1). The seism occurred along the North Anatolian Fault and caused numerous casualties (~17 000 deaths) and heavy damages in one of the most industrialized zones of the country, near the İzmit city. Field observations pertaining to geologic aspects of this disaster named as İzmit earthquake are reported in numerous works (Barka *et al.* 2002, Fukushima *et al.* 2002, Lettis *et al.* 2002, US Geological Survey (USGS) 2004). One of the environmental damages the earthquake caused (e.g. Eguchi *et al.* 2000) is the fire in the Tüpraş oil refinery (figure 2). Recent studies based on the aftershock distribution, radar interferometry, high-resolution satellite imagery and optimization of Global Positioning System (GPS) measurements have concluded that the earthquake fault terminated offshore somewhere at the north-east of Yalova town (see figures 2 and 4) (Feigl *et al.* 2002, Hearn *et al.* 2002, Michel and Avouac 2002, Polat *et al.* 2002). Recently, Kuşçu *et al.* (2005) used high-resolution seismic data to show that in the easternmost offshore part of the Gulf of İzmit, the amount of gas seeping from the seabottom increased after the 1999 earthquake.

Thermal infrared (TIR) anomalies observed in satellite imagery are recognized to be associated with earthquakes (Quing *et al.* 1991, Tronin 1996, 2000, Nosov 1998, Qi-Qi *et al.* 2000, Carreno *et al.* 2001, Tronin *et al.* 2002, Bryant *et al.* 2003, Fizzola

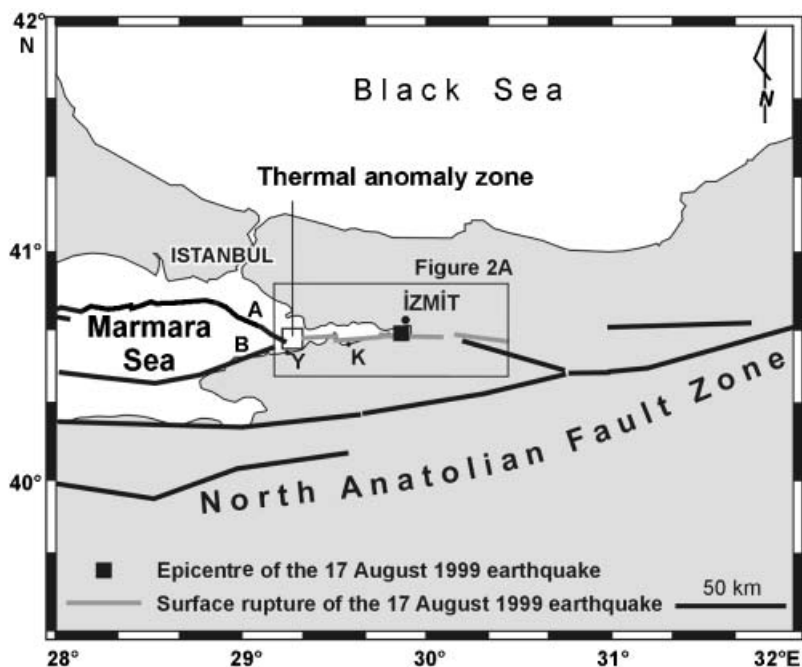


Figure 1. Map showing the area where the thermal infrared anomaly is observed. The fault segments ruptured during the 17 August 1999 earthquake are drawn based on data by Michel and Avouac (2002). The epicentre location is from USGS (2005). The North Anatolian Fault zone deviates at where the anomaly develops. B is the westerly propagation of the fault zone according to Le Pichon *et al.* (2001) whereas in the map of Armijo *et al.* (1999), the fault zone extends along segments A and B. K: Karamürsel; Y: Yalova.

*et al.* 2004, Ouzounov and Freund 2004, Tramutoli and Pietrapertosa 2005). When viewed in a Landsat Thematic Mapper (TM) satellite image acquired the next day after the earthquake (18 August 1999), the western parts of the disaster zone display a pronounced offshore anomaly in TIR band (figures 2, 3 and 4). In other satellite images (figure 3), in particular in the image acquired a week before the earthquake (figure 3(c)), this anomaly is not observed. The purpose of this paper is to present this anomaly, its geometry, physical significance and possible origin to discuss whether a relationship between the anomaly and the earthquake could be established. Such a study is important because this domain is not much explored, and it may provide valuable information to seismic research in tectonically active areas, in particular in zones where relatively shallow waterbodies are present.

## 2. Geological setting

The earthquake is generated along the North Anatolian Fault (NAF), considered as transforming-type plate boundary between the westerly moving Anatolian micro plate and the northern Eurasian plate (e.g. Şengör 1979). The fault is morphologically well marked by numerous structural valleys, fault splays, pull-apart basins and restraining zones (Barka and Kadinsky-Cade 1988). The İzmit earthquake occurred in an area where the fault enters from the east the Marmara Sea (figures 1 and 2), one of the active basins of the fault zone. The thermal anomaly develops where the NAF deviates to follow one fault zone (segment A in figure 1)

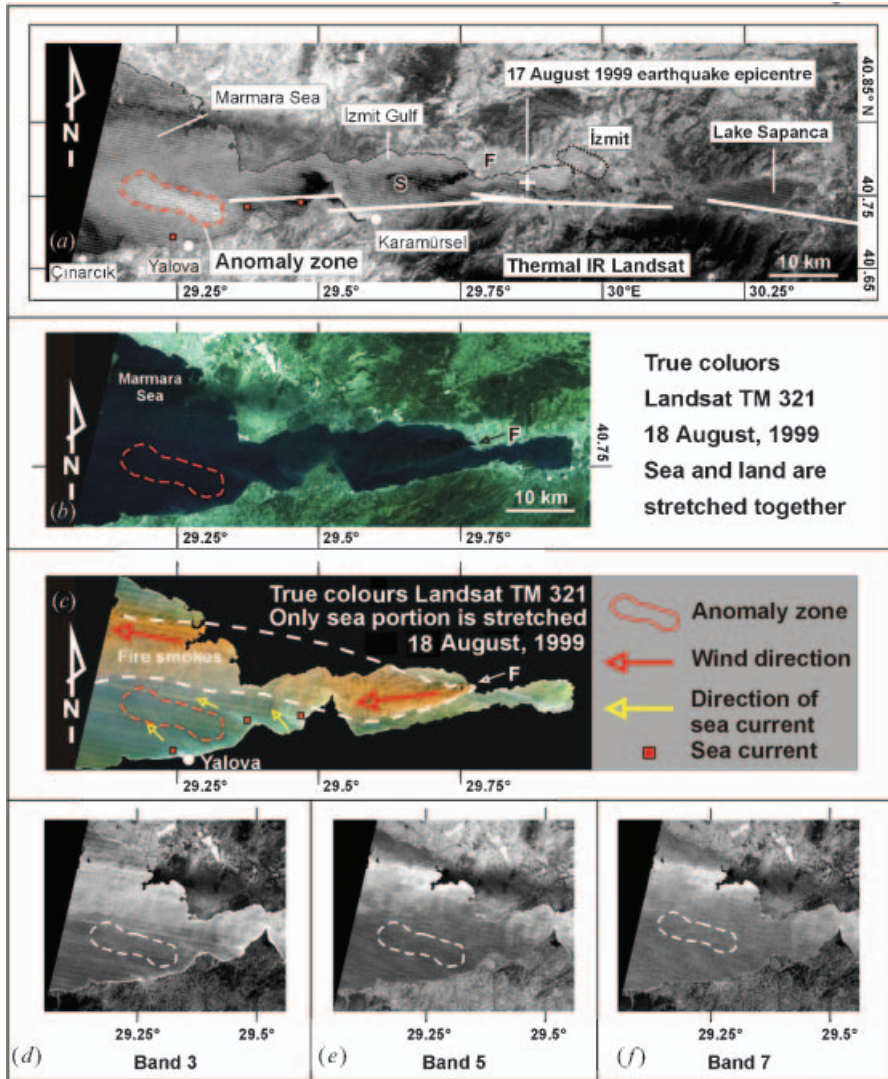


Figure 2. (a) Part of a Landsat TM (acquired on 18 August 1999) thermal infrared image showing the study area. The two waterbodies, the Marmara Sea at the west and the Sapanca Lake in the east, and the land are displayed after separately linearly stretching the raw data. At the west, the thermal anomaly zone is obvious in the sea whereas no anomaly is associated with Sapanca Lake. The epicentre of the 17 August 1999 earthquake is drawn according to USGS (2005) data. The heavy white lines depict the ruptured segments of the fault zone (Michel and Avouac 2002). Note that the anomaly zone develops where the earthquake fault ends. F: Tüpraş refinery fire. The black wedge (S) represents the fire smokes. (b) True-coloured Landsat composite image illustrating the Izmit Gulf, acquired the same day and obtained by linearly stretching and merging the first three bands (red: band 3; green: band 2; and blue: band 1). (c) Same image showing only the sea surface, and illustrating the extension of the fire smokes and sea currents. The three red points denote where sea currents are clear in the satellite image. These points are not associated with any thermal anomaly in the TIR image (marked as red points in (a)). (d) Band 3 of the Landsat TM data of 18 August 1999, showing the area in and near the thermal anomaly zone. Sea and land portions are stretched separately. The thermal anomaly zone is drawn as dashed white line. (e) and (f) Bands 5 and 7 of the same image, respectively, obtained using the same characteristics as in (d).

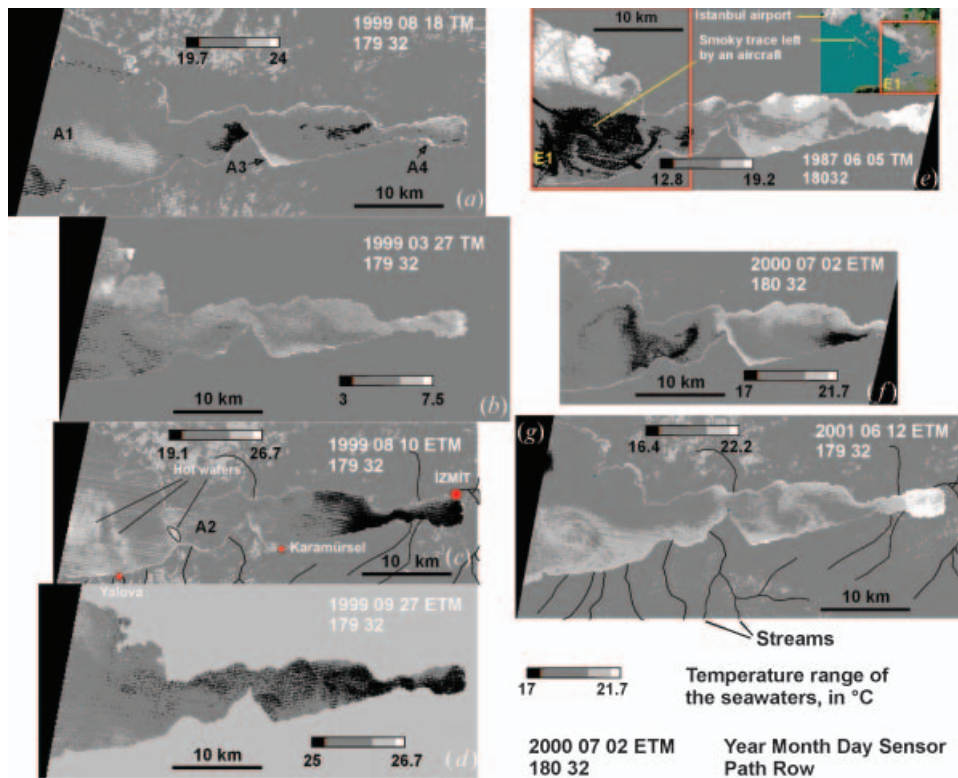


Figure 3. Partial Landsat TM or ETM satellite images showing the study area and adjacent zones in the thermal infrared spectral band. Sensor type, acquisition date, path and row of each image are shown in the right upper part of the image. Images acquired one day after (a), about five months prior to (b), one week prior to (c) and 40 days after (d) the 17 August 1999 earthquake. Digital data of both images are provided from the Eurimage Company (<http://www.eurimage.com>) immediately after the earthquake. (e), (f), (g) Other Landsat thermal infrared images of the study area. Source for this dataset of satellite images is the Global Land Cover Facility (<http://www.landcover.org>). E1: Colour composite image (red: band 3; green: band 2; and blue: band 1) of the western part of (e) that shows the smoky trace left by an aircraft having taken off from Istanbul airport.

towards the WNW (Le Pichon *et al.* 2001), or it splinters into this segment and another one (segment B in figure 1) extending towards the WSW (Armijo *et al.* 1999).

### 3. The western segment of the earthquake fault

Geophysical studies suggest that slip on the earthquake fault terminated somewhere in the Marmara Sea, at the north-east of Yalova town, a thermal spa known with its hot (64.5° C) thermo-mineral waters. The main shock was preceded by no foreshock activity and the only noticeable pre-seismic event was the formation of a new spring with waters with similar chemical characteristics, in the Yalova spa, on 2 August 1999 (Karagülle *et al.* 2000, Şimşek and Yıldırım 2000). The new spring is located on the same fracture zone as the older springs. Although earlier reports claimed temperatures reaching 80° C as well as soil deformations in the spa (Kırtay 1999), *in situ* measurements done several weeks after the earthquake (on 8 September) do

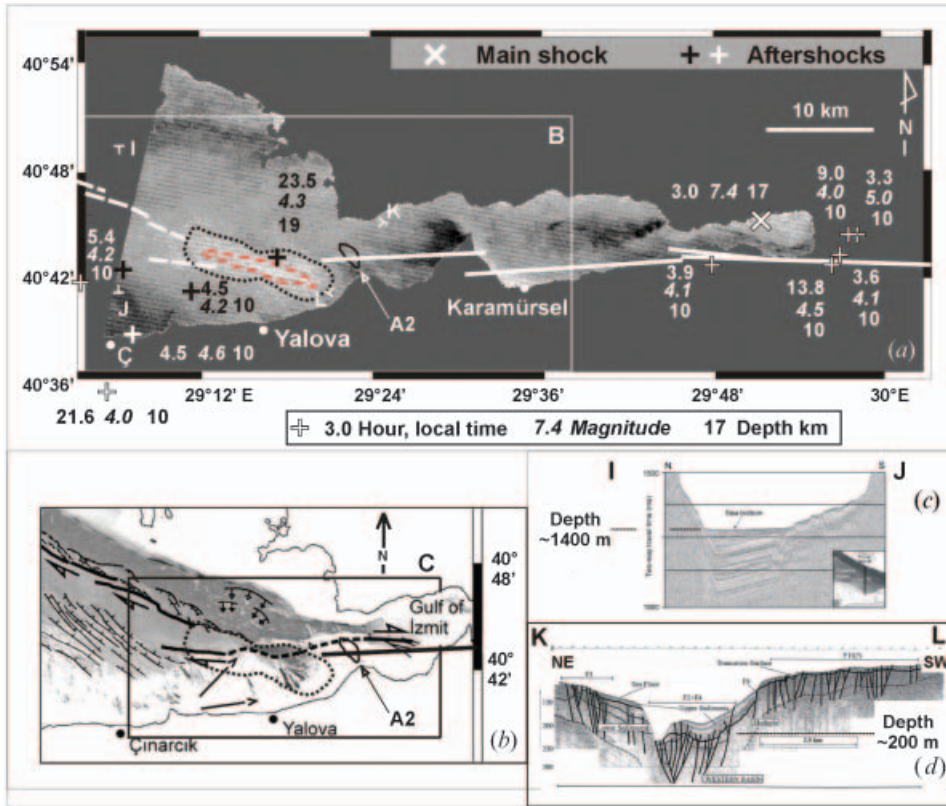


Figure 4. (a) Partial satellite image of the thermal infrared data anomaly in the Marmara Sea, illustrating only the sea surface after linear stretching of the Landsat TM data (band 6) acquired on 18 August 18 1999. Data source: Eurimage Company (<http://www.eurimage.com>). Fault segments ruptured during the earthquake are drawn with data from Michel and Avouac (2002). Main shock and aftershock epicentre locations which occurred prior to the satellite image acquisition on 18 August 1999 are from NEIC (2004). Ç: Çınarcık. Note that it is located near where the earthquake fault ended westerly. See text for A2. (b) Structural map of the Marmara Sea showing the submarine fractures and corresponding to the area around the anomaly zone (from Le Pichon *et al.* 2001). The two arrows at the lower central part denote the fracture zone that extends from the submarine canyon towards Yalova and that possibly channels the Yalova thermo-mineral waters. (c) Bathymetric map of the sea bottom beneath the anomaly zone (from Le Pichon *et al.* 2001). Cross-section of a (c) I–J profile (from Le Pichon *et al.* 2001) and (d) NE–SW profile, shown as K–L profile in (a) (from Gökaşan *et al.* 2001). These two profiles suggest a submarine canyon that deepens westwards and over which the positive anomaly developed.

not confirm these variations (Karagülle *et al.* 2000). The new source still delivers hot waters at a rate of 1 l/s.

#### 4. Data and method

The Gulf of İzmit and its near vicinity where the thermal anomaly is observed are pictured in several Landsat TM and Enhanced Thematic Mapper (ETM) images. The Landsat TM data for the anomaly day (18 August 1999) are cloud free (figure 2(b)) and atmospheric and surface conditions of that day do not present any particular condition (Ö. Dundar, meteorologist, Directorate of State Meteorological

Services, Ankara, personal communication). Satellite data are illustrated as documents of 120 m (for TM data) or 60 m (for ETM data) ground-resolution TIR images, and 30 m ground-resolution true colour composite images (TM data). In TIR images (figures 2, 3 and 4), the sea portion is extracted from the remaining land cover by automatic masking using band 4 data. This sea surface is linearly stretched to enhance the image for visual analysis. No other data manipulation such as atmospheric correction was performed on satellite data used. This is because: (1) no precise temperature estimations are needed in this study where a qualitative approach is performed; and (2) previous studies show that after atmospheric corrections, raw data and corrected data are reasonably well correlated for sea and lake surface temperatures (Chuang and Tseng 1998, Kay *et al.* 2005), meaning that temperature comparisons in one image can be done without significant errors. The digital number values of pixels of interest zones obtained from the TIR bands of satellite images are converted to temperature values using conversion formulas explained in the next section.

## 5. The thermal infrared anomaly

In the Landsat TM thermal infrared band acquired on 18 August 1999, an offshore anomaly appears at the north of Yalova town (figures 2(a), 3(a) and 4(a)). The anomaly has an elliptic, white-coloured central part with a WNW–ESE trending long axis of about 15 km length. Its width is about 5 km. The whitest part of the anomaly remains within the sea (figure 2(a)) and its light-coloured tones degrade to darker pixels when approaching the land, at the east and south-west (towards Çınarcık town). In the infrared band, the whiter tones correspond to the warmer surfaces of the Earth. In this brightest sector of the anomaly, the sea surface temperature is estimated to be 22.7° C whereas at the north of Çınarcık the sea surface has a temperature of about 21° C (computed according to Landsat 5 conversion formulations of TIR data to radiance and to ‘at-satellite temperature’ given by Chander and Markham 2004). This sector of the Marmara Sea is influenced by three events that affected the surface temperature on the day of data collection, namely this positive anomaly, a negative anomaly due to smokes that dissipated from the refinery fire in the east (figure 2(c)) and two positive anomalies along the seashore, one (A3 in figure 3(a)) at the west of Yalova and the other (A4 in figure 3(a)) at the eastern parts of the gulf (figures 2(a) and 3(a)). These last two anomalies form at the eastern faces of the seashore and may result from upwelling due to east wind (see figure 2 for the wind). The first two events, namely the positive anomaly at the north of Yalova and the anomaly associated with smokes, interfere near the northern parts of the anomaly leaving a narrow sea surface portion that is likely unaffected by these events. Lowest temperature values related to the positive anomaly will not be precise due to the interference of the northern anomaly. On the other hand, the western boundary of the satellite data (immediately at the west of Çınarcık town) does not allow one to speculate on how this anomaly affects the Sea of Marmara at the west. In conclusion, the 18 August TIR data suggest a difference of temperature of 1.7° C between the warmest (the central part) and coolest (at the north offshore of Çınarcık) parts of the anomaly. Absolute values cannot be given since neither at Yalova nor in the gulf do meteorological services operate temperature measurements. However, these relative estimations possibly are near real values in the warmest season of the year.

In other satellite data (figure 3(b)–(g)), this anomaly is not observed although these images are associated with different thermal anomalies that are discussed in the next section.

### 5.1 *Origin of the anomaly*

An anomaly of the TIR band means a temperature variation in the surface of the zone considered, the sea surface in this case. Such an anomaly may have different origins. In the TIR image of 18 August 1999, there is another anomaly easily detected with darker colours compared to the first anomaly (see figure 2(a) and (c)). This second anomaly runs at the eastern sector of the image, initiating in the shoreline from a small and very bright point in the land (F in figure 2(a)–(c)), where corresponding pixels are saturated in digital numbers (pixel values at 255) meaning that high temperatures existed in that zone. The anomaly trends ESE–WSW and loses its dark colour as its boundaries increase in surface (see figure 2(c) for the extension of the smokes). This anomaly corresponds to the fire (bright land point) the Tüpraş oil refinery caught and from which dark-coloured smokes emanated westwards drifted by the wind. The dark colour of the smokes suggests low temperatures (computed to 20° C) as expected since smokes usually have the temperature of the air independently of the source.

In figure 3 where several thermal band images are presented, some rather rectilinear anomalies are observed. In the Landsat ETM image acquired seven days before the earthquake, or on 10 August 1999, an alternation of hot and cold waters is observed as bands almost perpendicular to the seashore at the north of Yalova (figure 3(c)). Unlike the positive thermal anomaly discussed in the 18 August data, anomalies of this date seem to reach the shoreline, and may have originated from the land. The hot and cold waters have temperatures of 21.5° and 20.3° C, respectively, whilst the eastern parts of the Gulf of İzmit contain much colder waters (19.1° C) (temperatures computed using conversion formulations for ETM thermal band data from Landsat 7 2004). In the case of anomalies at the north of Yalova, the hot waters are likely those brought by rivers draining moderate heights (about 1000 m) at the south of the seashore. This explanation is not valid for the eastern positive anomaly A2, which developed in a zone where streams do not reach the sea. More to the east, the eastern tip of the gulf contains waters associated with colours darkening eastwards. This suggests that the gulf receives colder waters from the east, possibly due to streams that drain more elevated highlands (about 1300–1600 m) and bring colder waters to the gulf. The temperature of the seawaters in the Gulf of İzmit is thus about 20.3° C, or lower. In figure 3(e), a pronounced NW-trending heavy black line corresponds to the smoky trace left by an airplane since the smoke and its shadow on the sea surface are clear in visible bands (see figure 3(e) E1). There are, however, some other small lineaments that are seen in the same image at the north of this smoky trace. They are not identified in visible bands and are unlikely traces left by sea crafts since such traces distinguished in visible bands are not discerned in the thermal band, due to the low spatial resolution (120 m) of the TM data in this spectral band, or they do not have a thermal signature. Therefore their origin remains undetermined.

Large vortex-shaped or mushroom-like anomalies are also seen in some images (figure 3(e)–(g) and to a lesser degree (d)). At this scale, they correspond possibly to the sea current movements generated by the relatively warmer gulf waters and the colder waters coming from the northern Black Sea.

In the case of the first anomaly of 18 August 1999, the brightest colours attest for an augmentation of the surface temperature. This may be caused by various phenomena, mostly due to oil spills or bio-organic activity. Oil slicks can be detected by TIR sensors (Mineral Management Service (MMS) 2004, Almond 2005). Thick oil appears in white in infrared data whereas intermediate thicknesses appear black and thin oil is not detectable. As the sea anomaly encompasses with a hot zone, the oil spill, if there is any, should be thick in the central parts of the anomaly and there are chances to depict it in the 600–700 nm region of the visible spectrum since its natural colour is brown. Oil also dampens the surface waves, modifying reflection from the surface, a phenomenon that has chances to be determined in the visible spectra. There is, however, no such anomaly in the corresponding visible band (band 3, 630–690 nm, Landsat 2004; see figure 2(d)) of the Landsat image where the area under investigation is atmospherically clear, the positive anomaly zone remaining out of where the fire smokes extended (figure 2(c)). Studying the Exxon Valdez slick, Stringer and co-workers (Stringer *et al.* 1992) noticed that the 7 and 5 bands of Landsat TM data offer more chances to separate the ‘oil pixels’ from ‘water pixels’ due to different spectral signatures these two domains have. They consequently proposed contrast stretching of the data to differentiate oil from water. The stretching of the corresponding TM bands (band 5, figure 2(e); band 7, figure 2(f)) for the area of interest does not give any result. On the other hand, the whitish hot colours of the anomaly gradually pass into darker colours, meaning that if the anomaly is due to oil spill, the darker parts correspond to where the oil thins. This suggests a very large contamination area reaching as north as Istanbul and such a phenomenon would certainly be detected and considered as a second sinister besides the earthquake.

Another cause that may change the sea surface characteristics is the algal or phytoplankton bloom. The presence of such an activity is easily detected in visible bands, in particular with the green colouring of the sea surface due to the absorption of the incident light energy in wavelengths corresponding to blue and red colours by both the water and phytoplankton (Bigelow 2004; see satellite images of algal blooms in lakes and seas in NASA 2004 and Lakesat 2004). In the case of the anomaly zone in the Marmara Sea, the normally stretched visible bands of the Landsat data (in figure 2(b) and not in figure 2(c) where only the sea is stretched and its surface appears everywhere in green colours) do not suggest such an activity.

The location of the anomaly, especially its whitest thus warmest parts that remain in the sea, strongly suggests a marine origin for the anomaly, discarding a land-linked phenomenon, like the turbidity on the sea generated by numerous earthquake-triggered landslides along or near the shoreline, possibly the light-coloured pixel zones depicted in the visible bands, like those at the north of Yalova (shown by red points in figure 2(c)).

It thus seems likely that this anomaly is linked with a phenomenon that caused the seawater heating from the internal parts of the sea. The warming of the sea surface may be explained by heat transfer from a source not very warm and close to the surface, or from a source that is warm and far from the surface. The most plausible source is the sea bottom, and in this case the source is at least for several tens of metres far from the surface if the anomaly is located in the marine shelf environment. The source should have been the focus of significant heat quantity added to the sea bottom so that the following heat transfer may raise the surface temperature for about 2°C.

## 5.2 Bathymetry of the sea bottom beneath the anomaly

Investigated previously by Turkish Oil Company (Siyako *et al.* 2000), geophysical exploration studies have recently been undertaken in the offshore parts of the Marmara Sea (Gökaşan *et al.* 2001, Le Pichon *et al.* 2001). On the bathymetric and structural maps available, the long axis of the anomaly zone is underlain by a submarine canyon trending WNW–ESE (figure 4(b)). At the western end of the thermal anomaly, the canyon has a direction trending almost E–W and is deep for about 1400 m (figure 4(c)) whereas at the east of the anomaly and where the 1999 earthquake fault terminated, the depth of the canyon is about 200 m (figure 4(d)). The eastern tip of the anomaly therefore corresponds to where the fault deviates and the sea floor significantly deepens.

## 5.3 Source type and transfer of the heat

The study area is under the influence of a major fracture zone, the North Anatolian Fault, along which several thermal points are aligned. One of them is the Yalova spa where thermo-mineral waters reach a temperature of  $\sim 65^{\circ}\text{C}$ . The source of the heat necessary to warm the sea surface may be in link with waters warming due to geothermic gradient and upwelling in a deep crustal fracture zone. The depth of the main shock is 17 km, and depths of two of the aftershocks close to the anomaly are 10 and 19 km. At these depths, the normal geothermic gradient of  $3^{\circ}\text{C}/100\text{ m}$  will increase to  $300^{\circ}\text{--}570^{\circ}\text{C}$  the ambient temperature. Ramsay and Huber (1983) explained that during a strong earthquake, fluids filling the cracks that formed in periods close to the earthquake in rocks adjacent to the fault zone are rapidly expelled in zones of lower pressures, and generally upwards, in the crust. This process, namely the seismic pumping (Sibson *et al.* 1975), is used to explain the formation of ore deposits found close to fracture zones in the crust. Recently, Cox and Ruming (2004) showed that gold ore deposit enrichments are associated with aftershock activity of major fault zones, in particular in areas where faults bend. The gold is brought by high-flow fluxes of hot auriferous fluids during the aftershock activity. In our case, a similar process may have mobilized large quantities of waters circulating deeply in the cracks of the fault zone and heated by the geothermic gradient (figure 5). During the seismic activity, these fluids are forced to uprise towards the sea bottom (figure 5(b)). Thermal plumes may transfer the heat likewise added to the sea to finally elevate its surface temperature (figure 5(c)). Among aftershocks localized near the anomaly zone, the epicentre of the latest one (the one at the north of Yalova) is located near where the earthquake fault segment terminated at the west (figure 4(a)). More to the west, the fault bends (Le Pichon *et al.* 2001) or it bifurcates (Armijo *et al.* 1999). This aftershock occurred at about 23.50 h local time of the earthquake day (17 August) and the satellite data will be acquired several hours after, in the daytime of the next day (on 18 August). If this is the aftershock that generated the anomaly as its position near to the fault bend or junction suggests, about 10 h duration separates the aftershock and the following seismic pumping process to finally generate the anomaly. Possibly later the anomaly has evolved if the process of heating the surface was ongoing during data acquisition, but this cannot be verified in the lack of data. It remains also unclear if the oval shape of the anomaly is due to the drifting of the upwelling warmer waters as a result of wind and current effects as detected in the visible bands, or if this shape

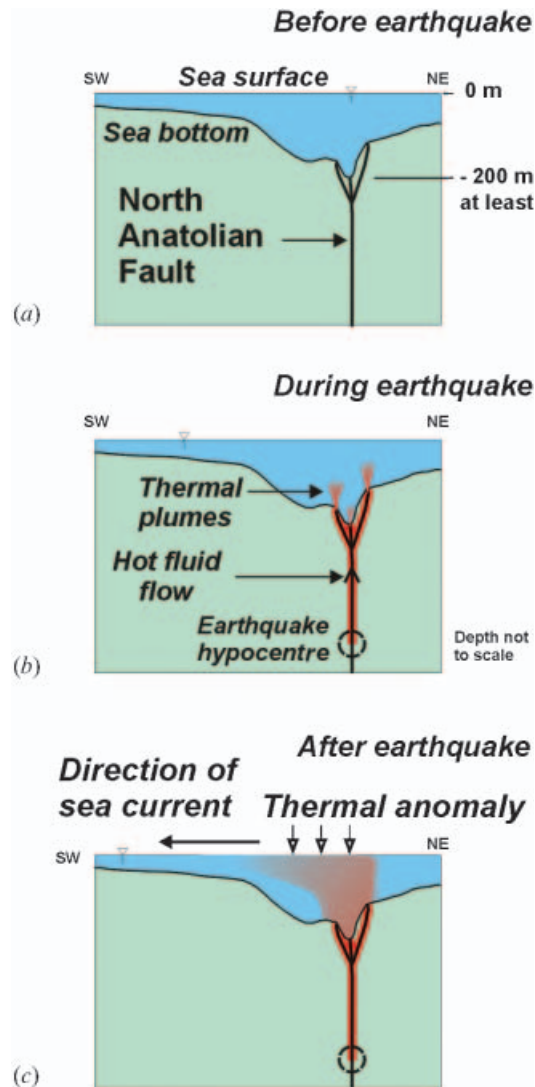


Figure 5. Schematic model depicting how the positive anomaly developed on the sea surface. Bathymetry is from Gökaşan *et al.* (2001). In (b), the earthquake causes fracturing along the fault surface. The shear stresses drop while the fluid pressure increases with the expulsion of the fluids heated due to geothermic gradient and trapped into the cracks of the faulting zone. Once these fluids reach the sea floor, they are upwelling towards the sea surface, producing the anomaly. (c) The elongate shape of the anomaly in map view may be inherited due to sea current activity and/or it may indicate that some length of the fracture beneath the anomaly is ruptured. Note that the current direction is not exactly towards the SW as is shown but towards the WNW (see figure 2(b)).

reflects the underlying fault zone from which waters reached the sea bottom along some fracture length.

## 6. Implications to seismologic phenomena

This study suggests that the temperature anomaly of the sea detected from satellite data originated from the sea, and may be due to the release of high volumes of hot

waters to the sea bottom during aftershock activity. For the fluids to uprise, this process necessitates the existence of open and interconnected fractures on their way up. This is possible if the whole crustal thickness remaining above the earthquake hypocentre is broken, suggesting that the earthquake caused some quantity of slip at the surface of the crust. This result is in agreement with those reached by SPOT image and radar interferometry analyses (e.g. Michel and Avouac 2002) for the onshore part of the earthquake fault. These tools are, however, not applicable to the offshore segments of the fault zone. Only the seismologic consideration of the aftershocks may shed light to which parts of the crust experienced fracturing but even this tool hardly predicts which quakes fractured the whole fault zone. If the explanation of the thermal anomaly by seismic pumping is true, the information that the whole crust beneath the anomaly underwent fracturing as deep as possibly to the hypocentre is an important conclusion and provides complementary data to the study of the earthquake under consideration.

The anomaly seems to form at the western termination of the earthquake fault. This zone may be the focus of future seismic activity as stresses are accumulated there following the 1999 earthquake. The WNW-trending fault segment that relays the 1999 earthquake fault (see figure 4(b)) is thought to be reactivated during the aftershock activity (Polat *et al.* 2002). Alternatively, studies of large-scale stress accumulation along NAF segments after the 1999 earthquake (*i.e.* Huber-Ferrari *et al.* 2000) indicate that zones prone to the next earthquake activity are in the northern segments of the fault zone. It therefore appears that in the future, the seismic activity will be produced in the marine environment of the Marmara region. This environment encompasses with deeper parts of the sea but also comprises relatively shallower marine sectors (Le Pichon *et al.* 2001). TIR satellite data that will be acquired in times near to the main shock of future activities may shed light to understand some parameters of the seismic phenomenon as those discussed in this study.

## 7. Conclusions

Landsat thermal infrared data analysis shows a positive temperature anomaly in the surface of the Marmara Sea in a zone where an earthquake fault has terminated, during the large August 1999 earthquake. The shape, location and formation time of the anomaly suggest a causative link with the earthquake formation. The anomaly is thought to develop by the rapid expulsion of large volumes of hot fluids circulating in the crust-scale fractures of the fault zone during the earthquake, and their upwelling from the sea bottom to finally elevate the surface temperature. The anomaly suggests the co-seismic rupture of the westernmost segment of the 1999 earthquake fault at the north of Yalova city during major and first aftershocks, or possibly during one aftershock that occurred on where the earthquake fault deviates. This information is of complementary value to other geophysical tools with regard to how far the earthquake fault propagated. The present work also suggests the fracturation of all the crustal thickness remaining above the aftershock hypocentre, a result in agreement with that reached using tools like radar interferometry. Among other applications of the remote sensing such structural interpretation of satellite images or radar interferometry, the TIR data seem to provide information that may be used to understand or discuss some characteristics of the seismologic phenomena, particularly in areas where seismic faulting occurs in shallow aqueous environments.

### Acknowledgments

The author is grateful to his colleagues Dr Onur Köse, from the Yüzüncü Yıl University, Van, Turkey, and Dr Kenan Tüfekçi, from MTA, for allowing him to use satellite data the Eurimage Company provided after the 1999 İzmit earthquake. Dr Orhan Gökdemir, from Hacettepe University, converted some satellite data to bitmaps. The author is grateful to his colleague Dr Yurdal Genç, from Hacettepe University, for his very constructive remarks and criticism. The author also would like to thank Professor Arun Saraf and two anonymous referees whose suggestions and comments improved the manuscript.

### References

- ALMOND, S., 2005, The remote sensing of oil slicks from satellite platforms. Available online at: <http://www.geog.ucl.ac.uk/~salmond/essay.html#tir> (accessed 14 January 2005).
- ARMIJO, R., MEYER, B., HUBERT, A. and BARKA, A., 1999, Westward propagation of the North Anatolian Fault into the northern Aegean: timing and kinematics. *Geology*, **27**, pp. 267–270.
- BARKA, A.A. and KADINSKY-CADE, K., 1988, Strike-slip fault geometry in Turkey and its influence on earthquake activity. *Tectonics*, **7**, pp. 663–684.
- BARKA, A., AKYÜZ, H.S., ALTUNEL, E., SUNAL, G., ÇAKIR Z., DİKBAŞ, A., YERLİ, B., ARMIJO, R., MEYER, B., DE CHABALIER, J.B., ROCKWELL, T., DOLAN, J.R., HARTLEB, R., DAWSON, T., CHRISTOFFERSON, S., TUCKER, A., FUMAL, T., LANGRIDGE, R., STENNER, H., LETTIS, W., BACHHUBER, J. and PAGE, W., 2002, The surface rupture and slip distribution of the 17 August 1999 İzmit earthquake (M 7.4), North Anatolian fault. *Bulletin of the Seismological Society of America*, **92**, pp. 43–60.
- BIGELOW, 2004, Toxic and harmful algal blooms, Bigelow Laboratory for Ocean Sciences. Available online at: <http://www.bigelow.org/hab/color.html> (accessed 2 March 2005).
- BRYANT, N., LOGAN, T.L., ZOBRIST, A.L., BUNCH, W.L. and NATHAN, R.B., 2003, Observed weather satellite thermal response prior to and after earthquakes. *Fall AGU 2004*, San Francisco, 9–12 December 2003, Abstract T52D-04. Available online at: <http://www.agu.org/cgi-bin/sessionsfm03?meeting=fm03&part=T52D> (accessed 1 December 2005).
- CARRENO, E., CAPOTE, R. and YAGUE, A., 2001, Observations of thermal anomaly associated to seismic activity from remote sensing. General Assembly of European Seismology Commission, Portugal, pp. 265–269.
- CHANDER, G. and MARKHAM, B., 2004, Revised Landsat 5 TM radiometric calibration procedures and post-calibration dynamic ranges. Available online at <http://landsat7.usgs.gov/documents/L5TMCAL2003.pdf>.
- CHUANG, H.-H. and TSENG, R.-S., 1998, Remote sensing of SST around the outfall of a power plant from Landsat and NOAA satellite. *Journal of Photogrammetry and Remote Sensing*, **3**, pp. 17–45 (in Chinese). Available online at: <http://www.gisdevelopment.net/aars/acrs/1998/ts2/ts2006pf.htm>.
- COX, S.F. and RUMING, K., 2004, The St Ives mesothermal gold system, Western Australia—a case of golden aftershocks? *Journal of Structural Geology*, **26**, pp. 1109–1125.
- EGUCHI, R.T., HOUSHMAND, B., HUYCK, C.K., MANSOURI, B., MATSUOKA, M., SHINOZUKA, M., YAMAZAKI, F. and ÜLGEN S., 2000, Using advanced technologies to conduct earthquake reconnaissance after the 1999 Marmara earthquake. Presented at the *2nd Workshop on Advanced Technologies in Urban Earthquake Disaster Mitigation*, DPRI, Kyoto University, Uji, Kyoto, Japan, 11–13 July 2000. Also available at: [imagecatinc.com/reportspubs/mamarappr.pdf](http://imagecatinc.com/reportspubs/mamarappr.pdf).
- FEIGL, K., SARTI, F., VADON, H., MCCLUSKY, S., ERGINTAY, S., DURAND, O.P., BURGMANN, R., RIGO, A., MASSONNET, D. and REILINGER, R., 2002, Estimating

- slip distribution for the Izmit mainshock from coseismic GPS, ERS-1, RADARSAT, and SPOT measurements. *Bulletin of the Seismological Society of America*, **92**, pp. 138–160.
- FIZZOLA, C., PERGOLA, N., PIETRAPERTOSA, C. and TRAMUTOLI, V., 2004, Robust satellite techniques for seismically active area monitoring: a sensitivity analysis on September 7, 1999 Athens's earthquake. *Physics and Chemistry of the Earth*, **29**, pp. 517–527.
- FUKUSHIMA, Y., KÖSE, O., YÜRÜR, T., VOLANT, P., CUSHING, E. and GUILLANDE, R., 2002, Attenuation characteristics of peak ground acceleration from fault trace of the 1999 Kocaeli (Turkey) earthquake and comparison of spectral acceleration with seismic design code. *Journal of Seismology*, **6**, pp. 379–396.
- GÖKAŞAN, E., ALPAR, B., GAZIOĞLU, C., YÜCEL, Z.K., TOK, B., DOĞAN, E. and GÜNEYSU, C., 2001, Active tectonics of the İzmit Gulf (NE Marmara Sea): from high resolution seismic and multi-beam bathymetry data. *Marine Geology*, **175**, pp. 273–288.
- HEARN, E.H., BÜRGMANN, R. and REILINGER, R., 2002, Dynamics of İzmit earthquake postseismic deformation and loading of the Düzce earthquake hypocenter. *Bulletin of the Seismological Society of America*, **92**, pp. 172–193.
- KARAGÜLLE, M.Z., GÜN, K., BAŞAK, E., DEMİRTAŞ, H., YÜZBAŞIOĞLU, N., GÜRDAL, H. and UYSAL, B., 2000, Körfez Depremi ve Yalova Termalleri (The gulf earthquake and the Yalova thermals). *Bilim ve Teknik*, TÜBİTAK, August 2000, pp. 98–100. Available online at: <http://www.biltek.tubitak.gov.tr/dergi/00/agustos/korfez.pdf> (in Turkish).
- KAY, J.E., KAMPF, S.K., HANDCOCK, R., CHERKAUER, K., GILLESPIE, A.R. and BURGESS, S.J., 2005, Accuracy of lake and stream temperatures estimated from thermal infrared imagery. *Journal of the American Water Resources Association* (in press).
- KIRTAY, F., 1999, A precursor activity of the İzmit earthquake? *Cumhuriyet* (Turkish newspaper), 4 September 1999. Available online at: <http://www.angelfire.com/de2/zellele/sinyal.html> (in Turkish).
- KUŞÇU, I., OKAMURA, M., MATSUOKA, H., GÖKAŞAN, E., AWATA, Y., TUR, H., ŞİMŞEK, M. and KEÇER, M., 2005, Seafloor gas seeps and sediment failures triggered by the August 17, 1999 earthquake in the Eastern part of the Gulf of İzmit, Sea of Marmara, NW Turkey. *Marine Geology*, **215**, pp. 193–214.
- LANDSAT, 2004, Lake water clarity monitoring and analysis with satellite remote sensing at the University of Wisconsin–Madison. Available online at: <http://www.lakesat.org/galleryindex.php>.
- LANDSAT, 2004, Landsat Thematic Mapper Data. Available online at: [http://edc.usgs.gov/guides/landsat\\_tm.html](http://edc.usgs.gov/guides/landsat_tm.html).
- LANDSAT, 7, 2004, The Landsat-7 science data user's handbook. Landsat Project Science Office, NASA's Goddard Space Flight Center, Greenbelt, MD. Available online at: [http://ftpwww.gsfc.nasa.gov/IAS/handbook/handbook\\_htmls/chapter11/chapter11.html](http://ftpwww.gsfc.nasa.gov/IAS/handbook/handbook_htmls/chapter11/chapter11.html).
- LE PICHON, X., ŞENGÖR, A.M.C., DEMİRBAG, E., RANGIN, C., İMREN, C., ARMIJO, R., GÖRÜR, N., ÇAĞATAY, N., MERCIER DE LEPINAY, B., MEYER, B., SAATÇILAR, R. and TOK, B., 2001, The active Main Marmara Fault. *Earth and Planetary Science Letters*, **192**(4), pp. 543–560.
- LETTIS, W., BACHHUBER, J., WITTER, R., BRANKMAN, C., RANDOLPH, C.E., BARKA, A., PAGE, W.D. and KAYA, A., 2002, Influence of releasing step-overs on surface fault rupture and fault segmentation: examples from the 17 August 1999 İzmit earthquake on the North Anatolian Fault, Turkey. *Bulletin of the Seismological Society of America*, **92**, pp. 19–42.
- MICHEL, R. and AVOUAC, J.P., 2002, Deformation due to the 17 August 1999 İzmit, Turkey, earthquake measured from SPOT images. *Journal of Geophysical Research*, **107**, 10.1029/2000JB000102.
- MMS, 2004, Oil spill remote sensing: a review. Emergencies Science Division, Ottawa, Canada. Available online at: <http://www.mms.gov/tarprojects/154/154AX.pdf>.
- NASA, 2004, Earth observatory, Natural Hazards page. Available online at: [http://earthobservatory.nasa.gov/NaturalHazards/natural\\_hazards\\_v2.php3?img\\_id=11889](http://earthobservatory.nasa.gov/NaturalHazards/natural_hazards_v2.php3?img_id=11889).

- NEIC, 2004, Aftershock data obtained from [http://neic.usgs.gov/neis/epic/epic\\_rect.html](http://neic.usgs.gov/neis/epic/epic_rect.html).
- NOSOV, M.A., 1998, Ocean surface temperature anomalies from underwater earthquakes. *Volcanology and Seismology*, **19**, pp. 371–375.
- OUZOUNOV, D. and FREUND, F., 2004, Mid-infrared emission prior to strong earthquakes analyzed by remote sensing data. *Advances in Space Research*, **33**, pp. 268–273.
- POLAT, O., EYIDOĞAN, H., HAESSLER, H., CISTERNAS, A. and PHILIP, H., 2002, Analysis and interpretation of the aftershock sequence of the August 17, 1999 Izmit (Turkey) earthquake. *Journal of Seismology* (Special Izmit Issue), **6**, pp. 287–306.
- QI-QI, L., DING, J. and CUI, C., 2000, Probable satellite thermal infrared anomaly before the Zhangbei M=6.2 earthquake on Jan 10, 1998. *Acta Seismologica Sinica*, **13**, pp. 203–209.
- QUING, Z., XIU-DENG, X. and CHANG-GONG, D., 1991, Thermal infrared anomaly—precursor of impending earthquakes. *Chinese Science Bulletin*, **36**, pp. 319–323.
- RAMSAY, J.G. and HUBER, M.I., 1983, *The Techniques of Modern Structural Geology: vol. 1 Strain Analysis* (New York: Academic Press).
- ŞENGÖR, A.M.C., 1979, The North Anatolian transform fault: its age, offset and tectonic significance. *Journal of the Geological Society of London*, **136**, pp. 269–282.
- SIBSON, R.H., MOORE, J.M. and RANKIN, A.H., 1975, Seismic pumping—a hydrothermal fluid transport mechanism. *Journal of the Geological Society of London*, **131**, pp. 653–659.
- ŞİMŞEK, Ş. and YILDIRIM, N., 2000, Geothermal activity at 17 August and 12 November 1999 eastern Marmara earthquake region, Turkey. *IGA Meeting*, 6–7 March 2000, Antalya, pp. 1–9. Available online at: <http://www.angelfire.com/de2/zelzele/termal.html> (in Turkish).
- SIYAKO, M., TANIŞ, T. and ŞAROĞLU, F., 2000, Marmara Denizi'nin Aktif Fay Geometrisi (Active fault geometry of the Marmara Sea). *Bilim ve Teknik*, March 2000. Available online at: [www.biltek.tubitak.gov.tr/dergi/00/mart/marmara.pdf](http://www.biltek.tubitak.gov.tr/dergi/00/mart/marmara.pdf) (in Turkish).
- STRINGER, W.J., DEAN, K.G., GURITZ, R.M., GARBEIL, H.M., GROVES, J.E. and AHLNAES, K., 1992, Detection of petroleum spilled from the MV Exxon Valdez. *International Journal of Remote Sensing*, **13**, pp. 799–824.
- TRAMUTOLI, V. and PIETRAPERTOSA, C., 2005, Assessing the potential of thermal infrared satellite surveys for monitoring seismically active areas. The case of Kocaeli (İ) earthquake, August 17th, 1999. *Remote Sensing of Environment*, **96** (3–4), pp. 409–426.
- TRONIN, A.A., 1996, Satellite thermal survey—a new tool for the studies of seismoactive regions. *International Journal of Remote Sensing*, **17**, pp. 1439–1455.
- TRONIN, A.A., 2000, Thermal IR satellite sensor data application for earthquake research in China. *International Journal of Remote Sensing*, **21**, pp. 3169–3177.
- TRONIN, A., HAYAKAWA, M. and MOLCHANOV, O.A., 2002, Thermal IR satellite data application for earthquake research in Japan and China. *Journal of Geodynamics*, **33**, pp. 519–534.
- USGS, 2004, Brief report on the 17 August 1999 earthquake is available online at: <http://quake.wr.usgs.gov/research/geology/turkey/>; a report is available online at: <http://pubs.usgs.gov/circ/2000/c1193/c1193.pdf>.
- USGS, 2005, Significant earthquakes of the world for 1999, the August 17 event. Available online at: [http://neic.usgs.gov/neis/eqlists/sig\\_1999.html](http://neic.usgs.gov/neis/eqlists/sig_1999.html).